A Study on the Influence of Anchor Rods' Layout on the Uplift Resistance Characteristics of Inclined Anchor Short-Pile Foundations Based on FEA

Yiran Gao [1], Yiqing Zhang [2], Qiang Xie [3,4,*], Quan Liu [2], Tinglei Liu [5], Ting You [5], Xiang Fu [6], Jun Duan [3], Peiyuan Qin [3], Tao Yang [3] and Yucheng Chen [3]

[1] State Grid Economic and Technology Research Institute Co., Ltd., Beijing 102209, China
[2] State Grid Chongqing Economic Research Institute, Chongqing 401121, China
[3] School of Civil Engineering, Chongqing University, Chongqing 400045, China
[4] National Joint Engineering Research Center of Geohazards Prevention in the Reservoir Areas (Chongqing), Chongqing 400045, China
[5] State Grid Chongqing Shinan Electric Power Supply Branch, Chongqing 400015, China
[6] School of River and Ocean, Chongqing Jiaotong University, Chongqing 400074, China
* Correspondence: xieqiang2000@163.com

Abstract: In the steep terrain of southwestern China, there are numerous complex strata characterized by thin overburden layers and well-behaved underlying bedrock, yet excavation poses significant challenges. This situation is unfavorable for the construction of transmission towers' foundations. To address this issue, inclined anchor short-pile foundations have been proposed as foundations for transmission towers. These foundations not only reduce the depth and construction difficulty of excavation but also make full use of the load-bearing capacity of the bedrock. To investigate the influence of the anchor rods' layout on the uplift resistance characteristics of inclined anchor short-pile foundations, numerical models were established using FLAC3D. The effects of the anchor rods' position and the length of the free segment on the uplift resistance characteristics of inclined anchor short-pile foundations were explored. The results indicated that variations in the anchor rods' position and the length of the free segment had minimal impact on the uplift resistance characteristics of inclined anchor short-pile foundations. The pile head displacements of short piles with different anchor rod positions were similar under both loading conditions. Under pure uplift loads, the maximum displacement before failure was approximately 13 mm, while under combined uplift and horizontal loads, the maximum displacement before failure was around 15 mm. Placing the anchor rod too low increased the difficulty of construction, while positioning it too high resulted in a shorter embedment length of the anchor rod in the pile's body, leading to potential failure at the pile–anchor node. Therefore, it is recommended to position the anchor rod near the center of the short pile's body. As the length of the free segment of the anchor rod decreased, there was a slight reduction in the displacement under the same uplift loading conditions, with an overall difference of less than 5%. However, if full-length anchoring was adopted, the anchor rod was prone to tensile shear failure. Compared with short-pile foundations of the same size, inclined anchor short-pile foundations demonstrated enhanced ultimate bearing capacity under uplift and combined uplift and horizontal loading. The improvement was more significant when horizontal loads were present. Under horizontal loading, the ultimate uplift bearing capacity of inclined anchor short-pile foundations decreased by only 14%, whereas that of single-pile foundations decreased by 24%.

Keywords: inclined anchor short-pile foundations; FLAC3D; uplift resistance characteristics; anchor rod layout; anchor rod position; length of the free segment

1. Introduction

As the economy of China rapidly develops, the scale of the power grid continues to expand, making the construction of transmission lines the norm in future substation

projects. However, in regions such as the southwestern mountainous areas of China, the presence of numerous complex terrains and rocky strata poses significant challenges to construction. Difficulty in construction arises from the complexities inherent in these terrains, making drilling a formidable task. Consequently, the construction of foundations for transmission towers encounters formidable challenges.

In the mountainous regions of China, various types of foundations, such as bored pile foundations [1], rock-embedded foundations [2], and rock anchor foundations [3], are predominantly utilized for power transmission lines. Extensive research has been conducted on the pullout bearing characteristics of these foundations. Li [4] proposed a multi-expansion-head bored pile foundation, comparing its load-bearing capacity and economic efficiency with traditional bored piles. The results indicated that under similar conditions, the multi-expansion-head bored pile foundation could enhance the pullout bearing capacity by 9% to 34%, while saving concrete by 4% to 26%. Zheng et al. [5] conducted field experiments to investigate the pullout performance of grouted bored piles, revealing a significant enhancement in the pullout bearing capacity through grouting. Wang et al. [6] utilized numerical simulation to calculate the pullout bearing capacity of bored piles on slopes, demonstrating a negative correlation between the pullout capacity and the slope ratio, and a positive correlation with foundation width or height, represented by a quadratic polynomial; however, when the slope ratio fell below a certain threshold, the capacity ceased to increase. Jiang et al. [7] studied the distribution of stress and the dissipation of deformation of rock-anchored bored-pile foundations under horizontal loads. Cui et al. [8] conducted field tests and analyzed the load-displacement curves of bored piles under different vertical loads, revealing distinct characteristics in the curves' shapes. Jiang et al. [9,10] proposed a novel anti-pullout pile, namely a composite anchor pile, demonstrating its uniform distribution of stress, superior durability, and mechanical performance compared with other piles, along with a method for calculating the composite anchor pile's bearing capacity. Ji et al. [11] concluded from indoor model tests of rock-embedded anti-pullout piles on flat and sloped grounds that the slope's inclination negatively affects the bearings' deformation characteristics, with the impact increasing with the slope's steepness. Hong et al. [12] analyzed the pullout bearing performance and failure characteristics of rock-embedded foundations on the basis of in situ tests, obtaining significantly improved ultimate shear strength parameters compared with the existing standards. Wang et al. [13] established a pullout bearing model based on typical field tests, determining the optimal anchor rod angle and pullout bearing mechanism for inclined anchor short piles. Cheng et al. [14] used finite element techniques to study the pullout bearing capacity of strip plate anchor foundations in sandy soils, laying a theoretical foundation for their application in sandy soil foundations. Sun et al. [15,16] proposed an anchor–pier foundation composed of pier foundations and a group of anchor foundations, analyzing the transmission mechanism of pullout and failure modes of the anchor–pier foundation through experiments, and providing a calculation method for the pullout coefficient. Wang et al. [17] proposed a method for determining the ultimate pullout bearing capacity of anti-pullout piles based on non-integral load-displacement curves obtained from field destructive tests. Chen et al. [18] designed a new type of rock anchor foundation based on a bonded-slip model for transmission lines, studying its mechanical properties under pullout and horizontal loadings, concluding that the foundation met the requirements of bearing capacity. Fang et al. [19] conducted model tests on pile extraction and the corresponding numerical simulations to investigate the mechanical parameters of both the pile and the surrounding soil under uplift loads. A novel expansive shell anchor proposed by Guo et al. [20] addressed the issue of insufficient load-bearing capacity due to failure modes such as anchor pullout. The study revealed that compared with conventional anchors, the new anchor significantly enhanced its resistance to uplift loads. Chen et al. [21], on the basis of existing calculation methods in the current specifications and considering the load characteristics of rock anchors, synthesized calculation methods for key issues such as the pullout capacity and fatigue life of anchors, providing values for the critical

parameters. Rahgozar et al. [22] investigated the influence of foundation models on the seismic response of low-rise controlled-rocking brace frames. A dynamic analysis and a fragility analysis were conducted to evaluate a set of sway prototypes under fixed and flexible conditions. Additionally, the effects of shallow foundations were compared with those of traditional brace frames on the sway prototypes. The results indicated that the controlled-rocking brace frame prototypes exhibited significant flexibility effects in the foundation. Younus et al. [23] determined the pulling capacity or resistance of basalt fiber reinforced polymer (BFRP) and glass fiber reinforced polymer (GFRP) sheet-wrapped piles by experiments. The results showed that, compared with unconstrained piles, the uplift resistance of the piles was improved greatly. Under dry conditions, the uplift resistance of BFRP and GFRP cladding was 35.56% and 15.56% higher than that of unconstrained piles, respectively. Ilamparuthi et al. [24] conducted an experimental study on the uplift behavior of a relatively large scale model of a round plate anchor with a diameter of up to 400 mm embedded in loose, medium density, and dense dry sand. It was found that the lifting capacity was greatly affected by the bolts' diameter, the embeddedness ratio, and the sand's density. The values of loose, medium, and dense sand were put forward as 4.8, 5.9, and 6.8, respectively, and the empirical equation they presented proved to be consistent with the facts. Drilled pile foundations and rock-socketed foundations impose less stringent geological requirements and have found wider application in engineering. However, due to their larger excavation volume, their construction difficulty and cost are high. Rock anchor foundations require less material and entail smaller excavations, thus lowering the construction difficulty, yet they demand higher geological conditions, resulting in a lower current application rate [25–28]. Compared with the aforementioned foundations, inclined anchor short-pile foundations exhibit complex structures, consisting of short-pile foundations and anchor rod structures, possessing good vertical load-bearing performance and enhanced anti-pullout characteristics. Moreover, with short construction periods and small amount of engineering, they are suitable for the complex geological conditions and mountainous terrain features of southwestern China [29]. Additionally, inclined anchor short-pile foundations are subjected not only to pure upward pullout loads but also to combined upward and horizontal loads, although the extent to which their anti-pullout bearing characteristics are influenced by the layout of the anchor rods remains unclear.

To address the aforementioned issues, this study used numerical simulation methods to investigate the influence of the anchors' layout configurations on the pullout bearing characteristics of inclined anchor short-pile foundations under composite loading conditions. Specifically, the study focused on the effects of the anchors' position and the length of the free segment. Various numerical models were constructed using FLAC3D (6.00) finite difference software, applying a controlled variable approach. Each factor's influence on the pile heads' displacement, bearing capacity, the axial force in the piles' body, and the load-bearing ratio of the anchor structure was analyzed under both upward pullout and combined upward–horizontal loading conditions. The findings elucidated the impact of the anchors' layout configurations on the pullout bearing characteristics of inclined anchor short-pile foundations, thus providing theoretical support for the construction of such foundations.

2. Numerical Modelling

FLAC3D software, which utilizes the explicit Lagrangian algorithm, was used for solving the dynamic equations of motion (including the internal variables) in the models. These equations were solved using an explicit approach, referred to as the "explicit solution". The explicit algorithm in FLAC3D offers several advantages: it demonstrates similar computational time for non-linear stress–strain relationships to linear constitutive models, while significantly reducing the computational cost compared with implicit solution strategies. Moreover, FLAC3D incorporates a hybrid discrete partitioning technique, enabling effective simulation of the material yield, plasticity, and large deformations in

the model. In this study, the numerical simulation involved the cooperative deformation of short piles and anchor structures in a skewed anchor short-pile foundation under loading conditions. The interactions among the pile's body, the anchor bars, and the soil, as well as the analysis of the forces, displacements, and material yield, are complex. Therefore, the finite difference method was used for efficient and rapid analysis in this numerical simulation.

All parameters in this study were derived from on-site static load tests of a single anti-pullout pile foundation in a certain engineering project [30] and the numerical model of the inclined anchor short-pile foundation was established using FLAC3D. According to the results of the on-site static load tests of the single anti-pullout pile, the deformation of the anti-pullout pile body was minimal, thus assuming the pile's body to be elastic and using an elastic model for modeling while neglecting plastic deformation. The Mohr–Coulomb constitutive model was selected for the rock mass. The Mohr–Coulomb constitutive model can better simulate the plastic failure of rocks, and its computational speed is relatively fast in numerical simulation analyses. The interaction between the pile and rock was simulated using the built-in zero-thickness interface elements in FLAC3D. These interface elements use the Mohr–Coulomb shear model, which is commonly used to analyze displacement and sliding between two solid elements. The parameters for calculating the numerical simulation were referenced from the geotechnical investigation report of the physical and mechanical parameters of the test site's rock and soil. The specific parameters are shown in Tables 1 and 2.

Table 1. Numerical simulation of the mechanical parameters of the rock and soil mass and the pile's body.

Solum	Weight (kN/m³)	Cohesive Strength (kPa)	Internal Frictional Angle (°)	Modulus of Elasticity (MPa)	Poisson Ratio
Medium-weathered muddy siltstone	24.0	580	38.8	480	0.35
Reinforced concrete pile	25.0	/	/	35,000	0.16

Table 2. Numerical simulation of the cell parameters of the contact surface.

Contact Surface Position	Normal Stiffness (GPa/m)	Tangential Stiffness (GPa/m)	Cohesive Strength (kPa)	Angle of Friction (°)
Medium-weathered muddy siltstone	50.2	50.2	522	31

In the inclined anchor short-pile foundation model presented in this study, the modeling of the anchor rod was achieved by combining solid elements and pile elements. The pile elements simulated the anchor bars, while the solid elements simulated the anchoring body, and the interface elements were used to simulate the sliding and displacement between the anchoring body and the rock mass. The choice of pile elements over cable elements was due to their bending resistance, enabling them to withstand certain horizontal forces. The length of the free segment of the anchor rod was 0.65 m, while the anchored segment's length was 4 m, featuring HRB400 hot-rolled ribbed steel bars with a diameter of 35 mm. The anchor bars were connected to the pile's body through bending. A structural model of the anchor rod is shown in Figure 1. The geometric and mechanical parameters of the pile's structural elements were determined on the basis of the corresponding parameters of the anchor rod and grouting material, as indicated in Tables 3 and 4.
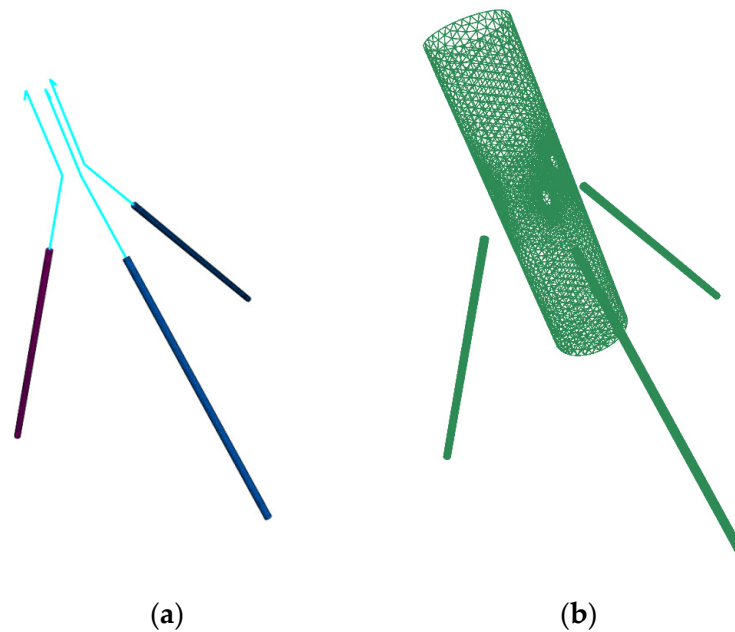
Figure 1. Schematic diagram of the anchor bolt's structure. (**a**) Schematic diagram of the model of the anchor rod. (**b**) Schematic diagram of the bolt's contact surface.

Table 3. Geometric and mechanical parameters of the pile's structural units.

Modulus of Elasticity (GPa)	Poisson Ratio	Pole Body Area (m^2)	Y axial Moment of Inertia (m^4)	Z Axial Moment of Inertia (m^4)	Polar Moment of Inertia (m^4)	Yield Strength (kN)	Elongation at Breaking
201	0.3	9.6×10^{-4}	7.36×10^{-8}	7.36×10^{-8}	1.47×10^{-7}	384	14%

Table 4. The grouting's mechanical parameters.

Modulus of Elasticity (GPa)	Poisson Ratio	Tensile Strength (kPa)	Cohesive Strength (kPa)	Internal Frictional angle (°)	Weight (kN/m^3)
30	0.17	70	3.18×10^3	50	24

As shown in Figure 2, the dimensions of the rock–soil mass model were set at 12 m × 12 m × 10 m. Tetrahedral meshing was used. Grid refinement was applied to the pile's body, the rock mass around the pile, and the grouting body of the anchor rod. The maximum grid size was set to 0.2 m at the pile's body and 0.03 m at the grouting body of the anchor rod. Larger grid sizes were chosen at the boundaries of the strata, with a maximum size of 1 m at the edges of the rock mass model. This approach ensured computational accuracy while minimizing the computational time.

The simulation involves two loading conditions: pure upward pullout loading and combined upward–horizontal loading. In the pure upward pullout loading condition, a stepwise equal load increment method was used. The initial load was set at 424 kN, with subsequent increments of 212 kN until failure of the inclined anchor short-pile foundation was observed. In the upward–horizontal loading condition, the upward pullout load was identical to that in the pure upward pullout loading condition. The initial horizontal load was set at 100 kN, with subsequent increments of 50 kN. Both the upward and horizontal loads were applied in stress form through the pile's cap.
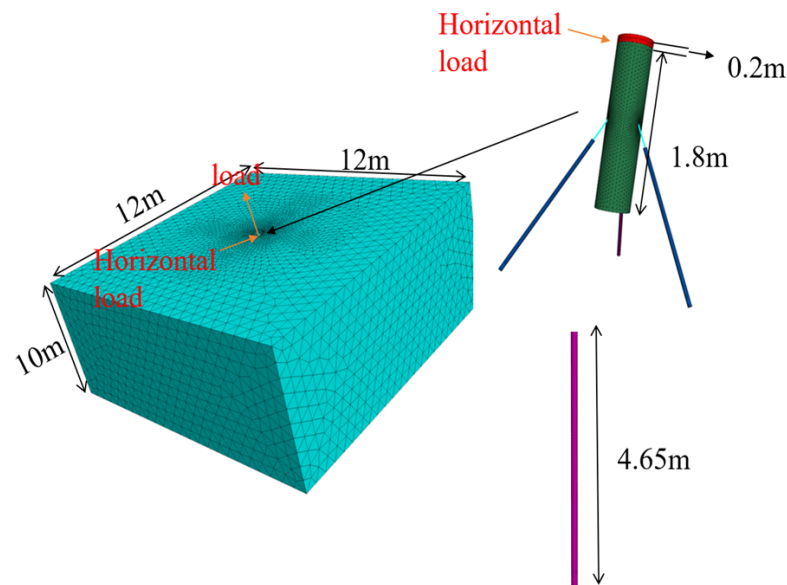
Figure 2. The model's mesh division.

The bottom boundary of the model was constrained in both the vertical and horizontal directions, while the side boundaries were constrained in the horizontal direction. The top boundary of the model was left unconstrained.

3. Numerical Results

3.1. Influence of the Anchor's Position

To investigate the impact of the anchor rod's position on the bearing capacity of inclined anchor short-pile foundations, numerical simulation models were established at distances of 0.6 m, 0.8 m, 1 m, 1.2 m, and 1.4 m from the ground surface. The analysis included various parameters, as shown in Table 5.

Table 5. Parameter setting of the anchor's position for analysis under working conditions.

Pile Length (m)	Anchor Diameter (mm)	Anchor Pole Angle (°)	Length of the Free Segment (m)	Horizontal Load
2	40	30	0.66	0.3 times lifting load

3.1.1. Displacement of the Pile's Top

As shown in Figure 3, under pure uplift loading conditions, the load-displacement curves of the inclined anchor short piles with five different anchor positions exhibited linear distributions before failure, with maximum displacements around 13 mm. Under uplift–horizontal loading conditions, the load-displacement curves displayed initial linear distributions in the early loading stages, followed by a decrease in the slope in the later stages of loading, with maximum displacements before failure averaging around 15 mm. Afterward, the failure of the short-pile foundation was observed. A significant increase in the pile's displacement occurred, resulting in the reinforcement within the free section of the anchors reaching fracture strain. This led to structural failure of the anchors. Consequently, the inclined anchor short-pile foundation experienced complete failure with substantial displacement.
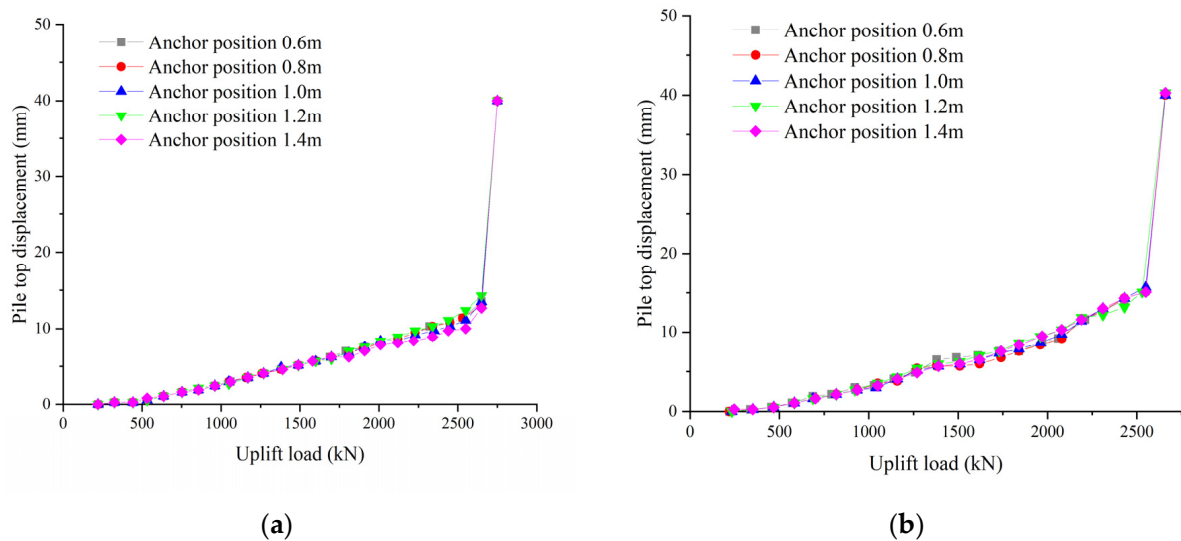
(a)

(b)

Figure 3. Load displacement curve of the inclined anchor short-pile foundation with different bolt positions: (**a**) uplift load; (**b**) uplift–horizontal load.

3.1.2. Bearing Capacity

Figure 4 presents the uplift capacity curves of inclined anchor short-pile foundations with pile–anchor nodes located at distances of 0.6 m, 0.8 m, 1 m, 1.2 m, and 1.4 m from the pile's top. Under pure uplift loading conditions, all five different anchor positions experienced failure upon reaching a load of 2650 kN. Under uplift–horizontal loading conditions, the uplift loads before failure were consistent at 2332 kN, indicating the minimal influence of variation in the anchor's position on the uplift capacity of inclined anchor short-pile foundations.
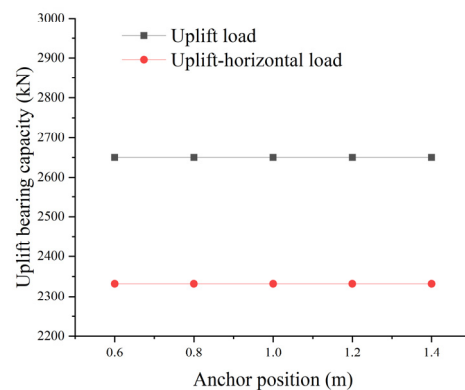

Figure 4. Influence of the bolt's position on the uplift bearing capacity of short-pile foundations with inclined anchors.

3.1.3. Axial Force of the Pile's Shaft

Figures 5 and 6 depict the variation in the axial along the pile's shaft for inclined anchor short-pile foundations with five different anchor positions under various uplift loads and uplift–horizontal loading conditions. Regardless of the loading conditions, similar trends in the variation in the axial force along the pile's shaft were observed for different anchor positions. Sharp decreases in the axial force occurred at the nodes' locations, and the slopes of the axial force curves beneath the nodes were nearly identical for different anchor positions. Above the nodes, the slope of the axial force curve increased with deeper anchor positions in the first half, while the slopes became similar in the latter half, indicating that the differences in the piles' resistance to sideways friction among the different anchor positions were significant only near the ground surface.
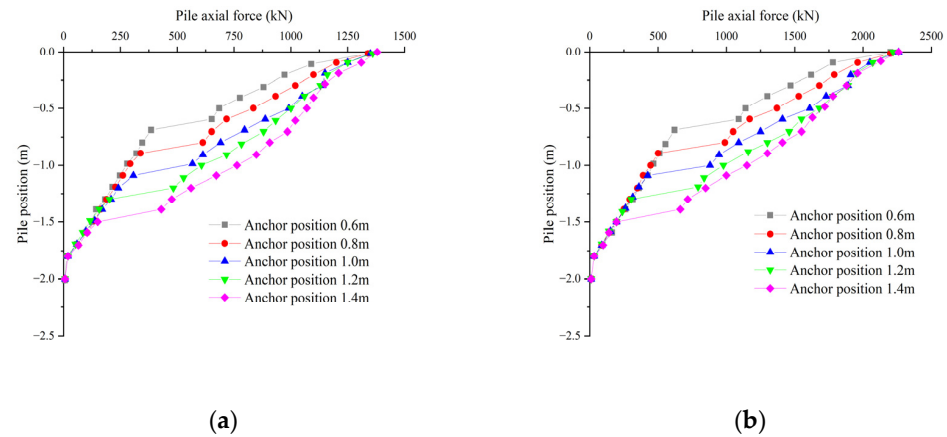
(**a**)   (**b**)

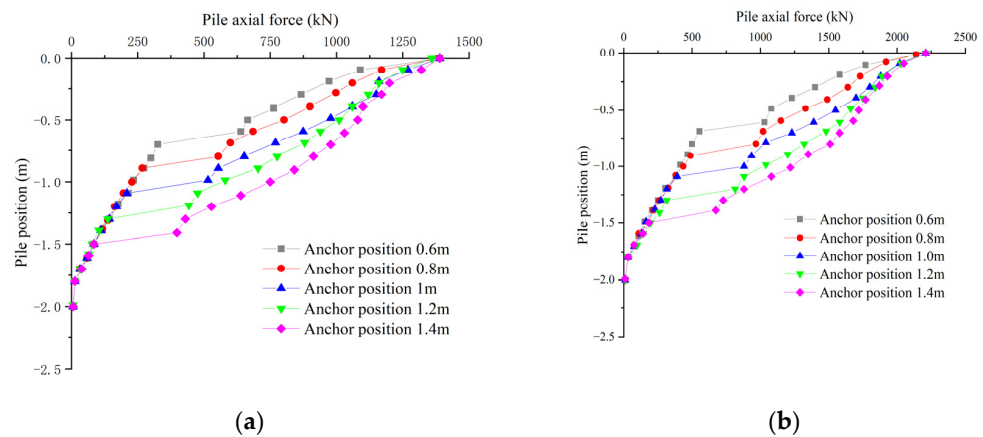**Figure 5.** Influence of the anchor's position on the axial force of inclined anchor short-pile foundation under the action of uplift load: (**a**) uplift load of 1378 kN; (**b**) uplift load of 2226 kN.

(**a**)   (**b**)

Figure 6. Influence of the anchor's position on the axial force of inclined anchor short-pile foundation under the action of uplift–horizontal load: (**a**) uplift load of 1378 kN; (**b**) uplift load of 2226 kN.

3.1.4. Load-Bearing Ratio of the Anchor Bolts' Structure

As shown in Figure 7, the development trend of the load-bearing ratio curves for the anchoring structures at different anchor positions remained consistent under both loading conditions. Therefore, the position of the anchor had a minimal impact on the load-bearing ratio of the anchoring structure for inclined anchor short-pile foundations under both pure uplift and uplift–horizontal loading conditions.
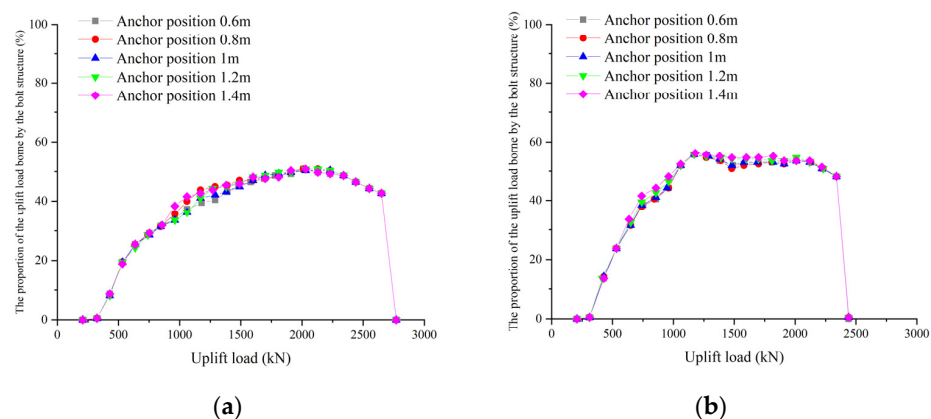

(**a**)   (**b**)

Figure 7. Influence of the bolts' position on the bearing ratio of the anchor bolts' structure: (**a**) uplift load; (**b**) uplift–horizontal load.

3.2. Influence of the Length of the Free Segment

To investigate the influence of the length of the anchor's free segment on the bearing capacity of inclined anchor short-pile foundations, numerical simulation models were established under conditions where the length of the anchor's free segment was 0 m, 0.33 m, 0.66 m, 0.99 m, and 1.32 m. Other parameters are listed in Table 6.

Table 6. Parameter setting of the length of the free segment for analysis under working conditions.

Pile Length (m)	Anchor Diameter (mm)	Anchor Node Position	Anchor Pole Angle (°)	Horizontal Load
2	40	Pile body in the point	30	0.3 times lifting load

3.2.1. Displacement of the Pile's Top

As depicted in Figure 8, under both loading conditions, the maximum displacement at the pile's top before failure remains almost consistent across the five curves. Throughout the loading process, except for the inclined anchor short-pile foundation with the fully anchored form, there was a slight increase in the displacement of the pile's top with an increase in the length of the anchor's free segment, although the overall difference was not significant. For the fully anchored form, during the early loading stages of both loading conditions, the displacement of the pile's top was less than that of the non-fully anchored form. However, as the loading progressed, the slope of the load-displacement curve increased, and ultimately, inflection points appeared at uplift loads of 2438 kN and 2014 kN, indicating failure of the inclined anchor short-pile foundation.
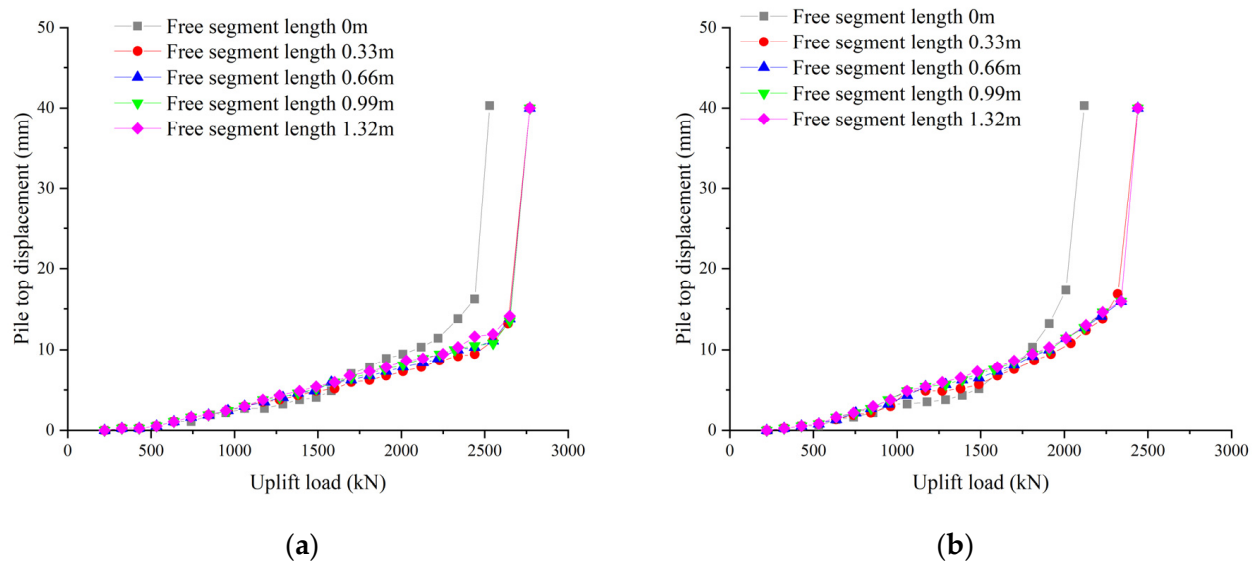

Figure 8. Load displacement curve of inclined anchor short-pile foundation with different lengths of the free segment: (**a**) uplift load; (**b**) uplift–horizontal load.

3.2.2. Bearing Capacity

As illustrated in Figure 9, as the length of the free segment increased from 0.33 m to 1.32 m, the foundations failed under pure uplift loading conditions upon reaching 2650 kN load, and under uplift–horizontal loading conditions, failure occurred at a 2332 kN load, indicating the minimal impact of the change in the length of the anchor's free segment on the bearing capacity of the inclined anchor short-pile foundation. If the anchor segment adopted a fully anchored form, the bearing capacity of the inclined anchor short-pile foundation decreased under both loading conditions. This can be attributed to the displacement between the grouting body at the pile–anchor node and the rock mass, resulting in the concentration of shear stresses in the anchor bars at the node, which progressively increased

with loading. Eventually, the anchor bars experienced shear failure, leading to a decrease in the uplift resistance of the inclined anchor short-pile foundation.
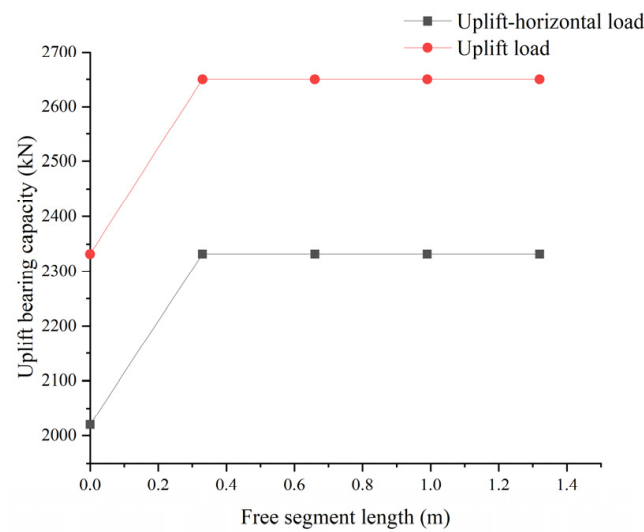

Figure 9. Influence of the length of the bolt's free section on the uplift bearing capacity of inclined bolt short-pile foundations.

3.2.3. Axial Force of the Pile's Shaft

As depicted in Figures 10 and 11, during the loading process, the axial force curves of the pile's body for the fully anchored form of the anchor exhibited steeper slopes beneath the node, indicating less displacement for the fully anchored inclined anchor short-pile foundation, resulting in reduced resistance of the pile to sideways friction beneath the node. The axial force curves for the length of the other four anchors' free segments almost overlapped, suggesting the minimal influence of changing the length of the anchor's free segment on both the axial force of the pile's body and the pile's resistance to sideways friction.
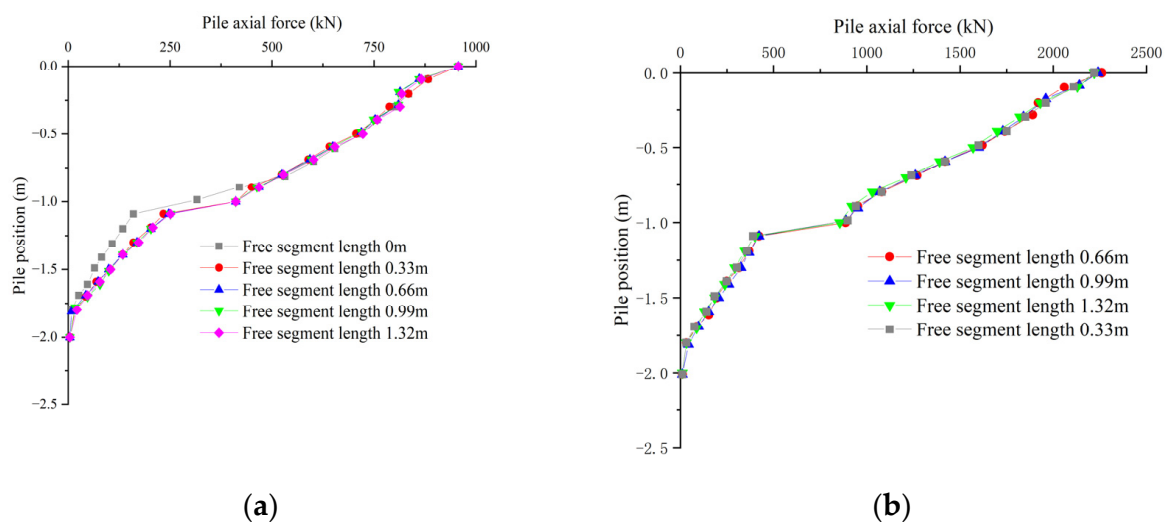

(**a**)

(**b**)

Figure 10. Influence of the length of the free segment on the axial force of the inclined anchor short-pile foundations under the action of uplift load: (**a**) uplift load of 956 kN; (**b**) uplift load of 2226 kN.
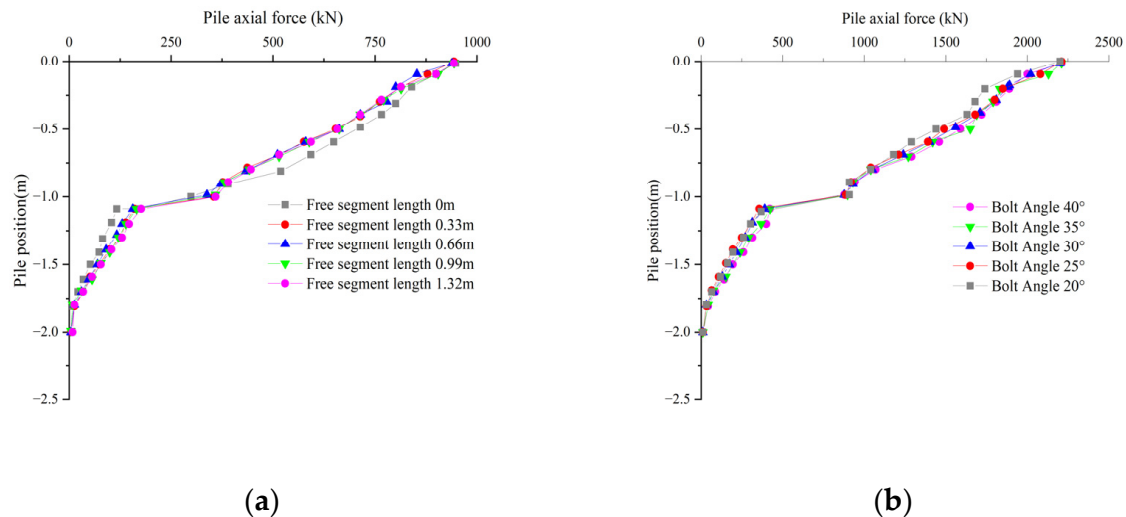
(**a**)   (**b**)

Figure 11. Influence of the length of the free segment on the axial force of inclined anchor short-pile foundations under the action of uplift–horizontal load: (**a**) uplift load of 956 kN; (**b**) uplift load of 2226 kN.

3.2.4. Load-Bearing Ratio of the Anchor Bolt Structure

As shown in Figure 12, the variation in the load-bearing ratio of the anchor structures for inclined anchor short-pile foundations with different lengths of the anchor's free segment remained similar during the loading process under both loading conditions. In the case of non-fully anchored forms of anchor, an increase in the length of the anchor's free segment resulted in a decrease in the load-bearing ratio of the anchor, indicating a reduction in the axial force of the anchor. As analyzed earlier, the change in length of the anchor's free segment had minimal impact on the displacement of the inclined anchor short-pile foundation. However, at the same node displacement, the load-bearing ratio of the anchor was inversely proportional to the length of the free segment of the anchor.
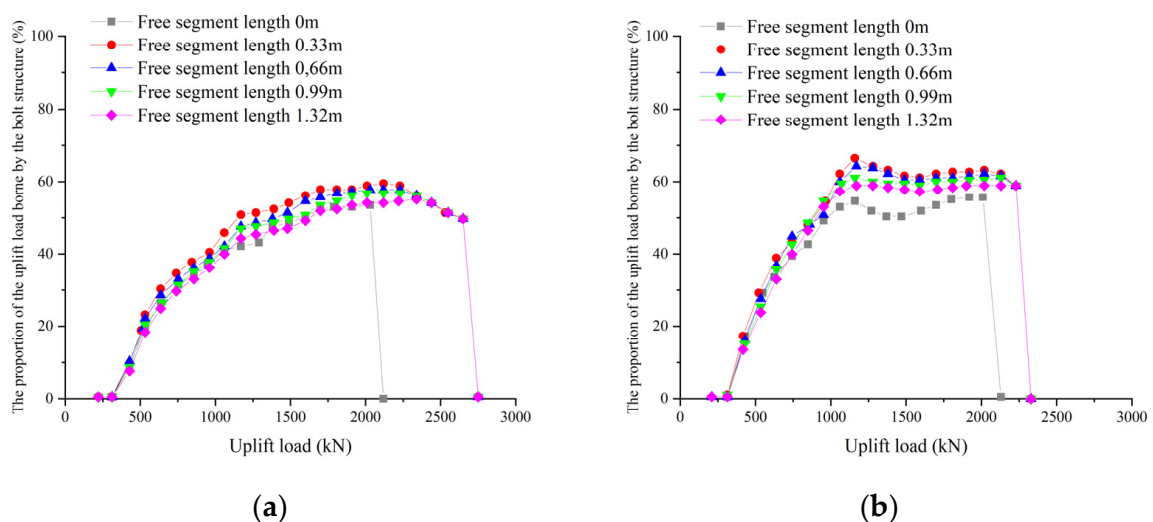

(**a**)   (**b**)

Figure 12. Influence of length of the free segment on the bearing ratio of the anchor bolt's structure: (**a**) uplift load; (**b**) uplift–horizontal load.

4. Discussion

Similar to the previous section, on the basis of the field static load test of a certain engineered anti-pulling single pile foundation, an embedded rock pile foundation model with equal sections was established to verify the advantages and rationality of the inclined anchor short-pile foundation.

In the numerical simulation of the anti-pulling embedded rock pile, the selection of constitutive models and parameters for the rock mass, pile body, and pile–rock contact surface was consistent with the selection in the numerical simulation of the inclined anchor short-pile foundation in the previous section. The model pile is shown in Figure 13.
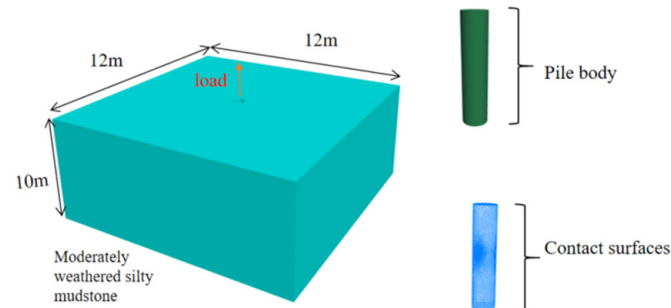

Figure 13. Numerical simulation model of the rock-socketed pile uplift test.

The simulation in this study used two loading conditions: pure uplift loading and uplift–horizontal loading, with the same loading method as in the previous section.

To investigate the effect of horizontal loading on the resistance to uplift of both the fully embedded single-pile foundations and the inclined anchor short-pile foundations, the load-displacement curves of the two types of pile foundations were analyzed, as shown in Figure 14.
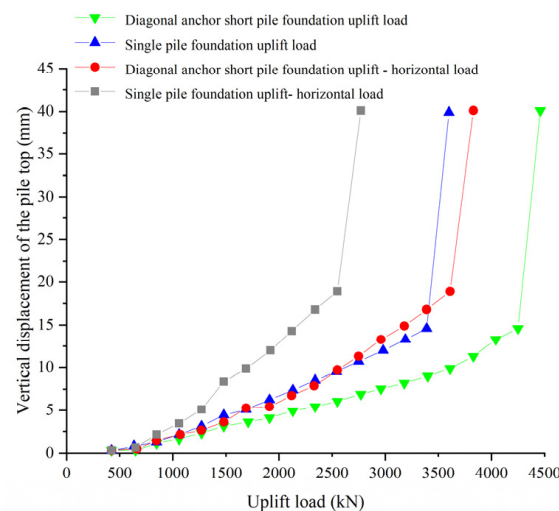

Figure 14. Vertical load displacement curve of the single-pile foundation and the inclined anchor short-pile foundation.

Under pure uplift loading conditions, the single-pile foundation failed when loaded to 3390 kN, with an ultimate uplift capacity of 3180 kN. The inclined anchor short-pile foundation, however, failed at 4244 kN, showing a significant increase in ultimate uplift capacity compared with the single-pile foundation, which was 3396 kN. The load-displacement curves of both the single-pile foundation and the inclined anchor short-pile foundation exhibited three segments: before reaching displacement of the pile's top of 13.3 mm, the curve showed gradual variation that was relatively gentle; from 13.3 mm to 14.6 mm, there was a slight increase in the slope but it remained linear; and when the displacement of the pile's top reached 14.6 mm, the single-pile foundation failed and the displacement increased substantially. For the inclined anchor short-pile foundation, before reaching displacement of the pile's top of 10.1 mm, the curve showed gradual variation that was relatively gentle, indicating elastic deformation of both the short-pile foundation and the anchoring structure. From 10.1 mm to 14.6 mm, the reinforcement of the anchor's foundation yielded, and

although there was a slight increase in the slope, the curve remained relatively gentle and linear. When the displacement of the pile's top reached 14.6 mm, which was the same as the ultimate displacement of the single-pile foundation, the short-pile foundation failed, with a substantial increase in the displacement of the pile's body, leading to the rupture strain of the reinforcement in the anchor's free segment, resulting in the failure of the anchoring structure and the overall failure of the inclined anchor short-pile foundation, accompanied by significant displacement. Compared with a short-pile foundation of the same size, the inclined anchor short-pile foundation exhibited an increased ultimate uplift capacity under uplift loading conditions, but the difference in the displacement of the pile's top between the two was not significant.

Under uplift–horizontal loading conditions, horizontal loading significantly affected the ultimate uplift capacity of both types of pile foundations. Specifically, the failure load of the single-pile foundation decreased from 3390 kN to 2550 kN, while that of the inclined anchor short-pile foundation decreased from 4244 kN to 3610 kN, with a smaller slope in the load-displacement curve. The load-displacement curve of the single pile foundation exhibited four segments: before reaching a displacement of the pile's top of 5.1 mm, the curve showed gradual variation that was relatively gentle; from 5.1 mm to 8.4 mm, there was a slight increase in the slope; from 8.4 mm to 18.9 mm, the slope decreased slightly but remained linear; and when the displacement of the pile's top reached 18.9 mm, the single-pile foundation failed, with a substantial increase in displacement. For the inclined anchor short-pile foundation, the load-displacement curve exhibited three segments: before reaching a displacement of the pile's top of 11.3 mm, the curve showed gradual variation that was relatively gentle, indicating elastic deformation of both the short-pile foundation and the anchor's structure; from 11.3 mm to 18.9 mm, the reinforcement of the anchor foundation yielded, and although there was a slight increase in the slope, the curve remained relatively gentle and linear; and when the displacement of the pile's top reached 18.9 mm, which was the same as the ultimate displacement of the single-pile foundation, the short-pile foundation failed, with a substantial increase in the displacement of the pile's body, leading to the rupture strain of the reinforcement in the anchor's free segment, resulting in the failure of the anchor's structure and the overall failure of the inclined anchor short-pile foundation, accompanied by significant displacement. Under uplift–horizontal loading conditions, the ultimate bearing capacity of the inclined anchor short-pile foundation improved compared with that of the single-pile foundation, and horizontal loading had a significant impact on the single-pile foundation. Compared with the single-pile foundation, the inclined anchor short-pile foundation, with its inclined anchor structure, could limit the inclination of the pile's body, thereby reducing the impact of horizontal loading on the uplift bearing capacity of the pile's body, with little difference in the displacement of the pile's top between the two.

In summary, under both pure uplift loading and uplift–horizontal loading conditions, the difference in the displacement of the pile's top between the inclined anchor short-pile foundation and the single-pile foundation was minimal, but the uplift resistance performance of the inclined anchor short-pile foundation was superior to that of the single-pile foundation. Under pure uplift loading conditions, there was only a slight increase of 216 kN in the ultimate uplift capacity of the inclined anchor short-pile foundation compared with the single-pile foundation. However, when subjected to horizontal loading, the ultimate uplift capacity of the inclined anchor short-pile foundation increased significantly to 1060 kN. Due to the synergistic loading of the anchor and the short pile in the inclined anchor short-pile foundation, the inclined anchor's structure can limit the inclination of the pile's body, thereby reducing the influence of horizontal loading on the uplift resistance of the pile's body. Its ability to withstand horizontal loading was significantly superior to that of the single-pile foundation.

5. Conclusions

This study used FLAC3D to investigate the effects of the anchor rods' position and length of the free segment on the uplift resistance characteristics of inclined anchor short-pile foundations under pure uplift and uplift–horizontal loading conditions. The distinctions between single-pile foundations and inclined anchor short-pile foundations are discussed, yielding the following main conclusions.

(1) The variation in anchor rods' position had a minimal impact on the uplift bearing characteristics of inclined anchor short-pile foundations. The displacements of the head of short piles with different positions for the anchor rods were similar under both loading conditions. Under pure uplift loads, the maximum displacement before failure was approximately 13 mm, while under combined uplift–horizontal loads, the maximum displacement before failure was around 15 mm. The development patterns of the load-bearing ratio curves for the anchor rod's structure were nearly identical. If the anchor rod was positioned too low, the difficulty of construction increased; conversely, if placed too high, the embedded length of the anchor bar in the pile was reduced, leading to potential failure at the pile–anchor node. Therefore, it is recommended to place the anchor rod near the center of the short pile's shaft.

(2) The variation in the length of the free section had a minimal effect on the uplift bearing characteristics of inclined anchor short-pile foundations. An increase in the free section's length resulted in only a slight increase in the displacement of the pile's head, with an overall difference of less than 5%. As the length of the free section decreased, the displacement of the inclined anchor short-pile foundation under the same uplift load decreased slightly, also by less than 5%. However, if full-length anchoring is used, the anchor bars may be prone to tensile shear failure.

(3) Compared with short-pile foundations of the same size, inclined anchor short-pile foundations demonstrated enhanced ultimate bearing capacity under uplift and combined uplift–horizontal loading. The improvement was more significant when horizontal loads were present. Under horizontal loading, the ultimate uplift bearing capacity of inclined anchor short-pile foundations decreased by only 14%, whereas that of single-pile foundations decreased by 24%. Although horizontal loads reduced the uplift bearing capacity of pile foundations, the inclined anchor structure in inclined anchor short-pile foundations mitigated the pile's inclination, thereby reducing the adverse impact of horizontal loads on the uplift bearing capacity.

In practical engineering, the loads experienced by transmission towers' foundations are random and unpredictable. These loads comprise complex periodic combinations of downward, upward, and horizontal cyclic forces. Since uplift capacity is a primary controlling factor for the stability of transmission towers' foundations, this study focused exclusively on the uplift loads and the combined effects of uplift–horizontal loads on the uplift capacity of inclined anchor short-pile foundations. Future research should consider the effects of combinations of downward, uplift, and horizontal cyclic loading on the bearing capacity of inclined anchor short-pile foundations.

Author Contributions: Data curation, methodology, and formal analysis, Y.G. and Y.Z.; methodology analysis and numerical analyses, Q.X., T.L., T.Y. (Ting You) and P.Q.; writing—original draft, T.Y. (Tao Yang) and Y.C.; literature collection, Q.L., X.F. and J.D. All authors have read and agreed to the published version of the manuscript.

Data Availability Statement: The original contributions presented in the study are included in the article. Further inquiries can be directed to the corresponding author.

Conflicts of Interest: Author Yiran Gao was employed by the company State Grid Economic and Technology Research Institute Co., Ltd. Authors Yiqing Zhang and Quan Liu were employed by the company State Grid Chongqing Economic Research Institute. Authors Tinglei Liu and Ting You were

employed by the State Grid Chongqing Shinan Electric Power Supply Branch. The remaining authors declare that the research was conducted in the absence of any commercial or financial relationships that could be construed as a potential conflict of interest.

References

1. Gong, Z.W. Discussion on some problems of hole pile foundation design. *Build. Struct.* **1996**, *10*, 50–55.
2. Wang, Y.H.; Zha, C.M.; Wang, H.T.; Li, C.Q.; Sun, J.W. Reinforcement treatment of rock embedded foundation for transmission line. *Electr. Power Surv. Des.* **2023**, *10*, 19–22.
3. Ye, G.; Liu, H.C.; Gu, L.Y.; Zhou, J.J.; Liao, X.J. Reliability analysis of rock anchor rod foundation for transmission line. *J. Wuhan Univ. Eng. Ed.* **2021**, *54*, 203–206.
4. Li, J.H. Application of multi-expansion pile foundation in transmission lines. *South. Energy Constr.* **2020**, *7*, 45–499.
5. Zheng, A.; Zhuge, A. Experimental study on bearing behaviour of different uplift piles. *IOP Conf. Ser. Earth Environ. Sci.* **2019**, *304*, 052013. [CrossRef]
6. Wang, X.Y.; Peng, B.; Tang, X.C.; Fan, L. Numerical Simulation for Uplift Bearing Capacity and Affecting Factors of the Digging Piles in Slope Ground. *Appl. Mech. Mater.* **2013**, *423–426*, 1292–1295. [CrossRef]
7. Jiang, Y.H.; Zhu, Z.D.; Sun, M.Q. Study on the stress distribution of surrounding rock when the artificial excavated pile foundation is subjected to horizontal load. *Electr. Power Surv. Des.* **2018**, *S1*, 6–11.
8. Cui, Q.; Yang, W.Z. Field test study on the bearing performance of transmission line bore pile under complex load conditions. *Chin. J. Geotech. Eng.* **2022**, *44*, 219–225.
9. Jiang, J.Q.; Mao, Z.Y.; Chen, L.H.; Wu, Y.K. Finite Element Analysis of Load-Bearing Characteristics and Design Method for New Composite-Anchor Uplift Piles. *Appl. Sci.* **2024**, *14*, 2100. [CrossRef]
10. Mao, Z.Y.; Jiang, J.Q.; Guo, H.; Wang, E.Z. Development and Mechanical Property Analysis of a Novel Uplift Pile Incorporating Composite Anchors. *Buildings* **2023**, *13*, 2029. [CrossRef]
11. Ji, Y.K.; Wang, Q.K.; Zhao, G.L.; Zhang, J.; Ma, J.L. Model test and numerical simulation of vertical bearing deformation characteristics of rock-socketed pile on slope. *Rock Soil Mech.* **2023**, *44*, 1604–1614.
12. Hong, T.X.; Zheng, W.F.; Ye, C. Study on key design parameters of rock embedded foundation for transmission lines. *J. Water Conserv. Constr. Eng.* **2018**, *16*, 150–155.
13. Wang, Y.H.; Yin, H.W.; Li, J.L.; Deng, H.F. Analysis and calculation of tensile bearing characteristics of inclined anchor composite foundation of short pile. *J. Archit. Sci. Eng.* **2023**, 1–12.
14. Cheng, L.; Niu, F.J.; Zhou, M.; Jiang, H.Q.; Xie, J.H. Bearing capacity of plate anchor foundation in sand foundation. *J. Harbin Inst. Technol.* **2022**, *54*, 126–134.
15. Sun, Y.Z.; Sun, H.L.; Tang, C.; Cai, Y.Q.; Pan, F. Monotonic uplift behavior of anchored pier foundations in soil overlying rock. *J. Zhejiang Univ. Sci. A* **2023**, *24*, 569–583. [CrossRef]
16. Sun, Y.Z.; Pan, K.; Tang, C.; Sun, H.L.; Sun, H.L. Field experimental study on cyclic uplift behavior of anchored pier foundations. *Acta Geotech.* **2022**, *17*, 4419–4434. [CrossRef]
17. Wang, Q.K.; Ma, J.L.; Ji, Y.K.; Zhang, J.; Chen, W.L. Using the complete and incomplete load-displacement curve to determine the ultimate bearing capacity of the resistant piles. *J. Cent. South Univ.* **2022**, *29*, 470–485. [CrossRef]
18. Chen, Z.; Gou, M.; Xu, W.Z.; Zhang, L.G.; Yang, X.J.; Yan, X.M. Research on the foundation design of new transmission line prefabricated rock bolt based on bond-slip model. *Adhesive* **2023**, *50*, 52–55.
19. Fang, J.P.; Lin, S.C.; Liu, K. Multi-scale study of load-bearing mechanism of uplift piles based on model tests and numerical simulations. *Sci. Rep.* **2023**, *13*, 6410. [CrossRef]
20. Guo, L.; Dong, X.A.; Wang, Z.; Li, H.; Song, Y.L. Field experimental study on the pull-out characteristics of a new type of expanding shell bolt. *Eng. Fail. Anal.* **2023**, *153*, 107571. [CrossRef]
21. Chen, J.L.; Wu, M.; Li, X.B. Research on the design method of rock anchor rod foundation of wind power generation tower. *Build. Struct.* **2017**, *47*, 86–90.
22. Rahgozar, N.; Rahgozar, N.; Moghadam, S.A. Controlled-rocking Braced Frame Bearing on a Shallow Foundation. *Structures* **2018**, *16*, 63–1672. [CrossRef]
23. Younus, M.M.M.; Murugan, M.; Singh, B.S. Uplift Behaviour of External Fibre-Reinforced Polymer Wrapping on RC Piles in Dry and Submerged Sandy Soil. *Buildings* **2023**, *13*, 778. [CrossRef]
24. Ilamparuthi, K.; Dickin, A.E.; Muthukrisnaiah, K. Experimental investigation of the uplift behaviour of circular plate anchors embedded in sand. *Can. Geotech. J.* **2002**, *39*, 648–664. [CrossRef]
25. Tong, R.M.; Lu, X.L.; Zheng, W.F. Experiment Study on Bolts Foundation of Large-Jointed Rock Mass in Transmission Lines. *Appl. Mech. Mater.* **2012**, *256–259*, 344–349. [CrossRef]
26. Wang, Y.H.; Wang, Y.H.; Liu, H.; Dong, D.; Cha, C.M. Type selection analysis of transmission line tower foundation. *Hebei Electr. Power Technol.* **2022**, *41*, 57–61.
27. Zhang, Y.; Zheng, W.F. Experiment Research of Rock Anchor Foundation on Sandstone Ground in Transmission Line. *Appl. Mech. Mater.* **2014**, *580–583*, 601–605. [CrossRef]
28. Zhang, X.G.; Huang, L.Y.; Wang, Y.; Wang, J.Q. Testing Methods for Rock-Embedded Foundation Pile in Karst Area. *Appl. Mech. Mater.* **2011**, *55–57*, 105–108. [CrossRef]

29. Li, Y.J.; Wu, X.Y.; Pu, D.P.; Shao, J.; Liao, X.; Xi, Y.W.; Peng, Y.L.; Ling, S.X. Analysis of karst hydrogeological structure type and groundwater dynamic characteristics in southwest mountainous area. *Subgrade Work.* **2020**, *6*, 13–18+24.
30. Yu, J.L. Numerical Analysis of Bearing Characteristics of Expanded Rock-Driven Pile. Master's Thesis, Nanchang Hangkong University, Nanchang, China, 2018.